2-D Finite Difference Time Domain Model of Ultrasound Reflection From Normal and Osteoarthritic Human Articular Cartilage Surface

Erna Kaleva, Jukka Liukkonen, Juha Töyräs, Simo Saarakkala, Panu Kiviranta, and Jukka S. Jurvelin

***Abstract*—Quantitative high-frequency ultrasonic evaluation of articular cartilage has shown a potential for the diagnosis of osteoarthritis, where the roughness of the surface, collagen and proteoglycan contents, and the density and mechanical properties of cartilage change concurrently. Experimentally, these factors are difficult to investigate individually and thus a numerical model is needed. The present study is the first one to use finite difference time domain modeling of pulse-echo measurements of articular cartilage. Ultrasound reflection from the surface was investigated with varying surface roughness, material parameters (Young's modulus, density, longitudinal, and transversal velocities) and inclination of the samples. The 2-D simulation results were compared with the results from experimental measurements of the same samples in an identical geometry. Both the roughness and the material parameters contributed significantly to the ultrasound reflection. The angular dependence of the ultrasound reflection was strong for a smooth cartilage surface but disappeared for the samples with a rougher surface. These results support the findings of previous experimental studies and indicate that ultrasound detects changes in the cartilage that are characteristic of osteoarthritis. In the present study there are differences between the results of the simulations and the experimental measurements. However, the systematic patterns in the experimental behavior are correctly reproduced by the model. In the future, our goal is to develop more realistic acoustic models incorporating inhomogeneity and anisotropy of the cartilage.**

I. Introduction

Osteoarthritis (OA) is a common degenerative musculoskeletal disease. The onset of OA is typically related to aging or mechanical injuries causing biomechanical, biochemical, and structural changes to the articular cartilage and subchondral bone [1]. Progressive OA is associated with an increase in the water content, depletion of the proteoglycans (PG) and disruption of the collagen matrix in the cartilage [2]–[5]. There is a lack of an efficient *in vivo* method for detecting the incipient signs of the OA in the early, possibly reversible, stages before the symptoms reveal the irreversible damage to the cartilage and bone.

Based on earlier experimental studies, high-frequency ultrasonic evaluation of the structure and mechanical properties of articular cartilage may become a clinically relevant diagnostic tool [6]–[14]. It has been experimentally revealed that increase in the roughness of the surface [11]–[13], [15], [16] and decrease in the collagen content [17] and density of the cartilage diminish the ultrasound reflection from the surface of the cartilage. In OA, all these factors are concurrent, and thus, evaluating the effects of changes in any individual factor is experimentally difficult. It is also known that the incident angle of the ultrasound beam on the cartilage affects the amplitude of the reflected ultrasound relatively more in intact than in degenerated cartilage [11], [16], [18]. A numerical model could enable the evaluation of the contributions of these factors. However, ultrasound reflection from the surface of the cartilage has not, to our knowledge, been modeled before, although the reflection and scattering phenomena in engineering materials have been explored widely.

In this study, we developed a sample-specific 2-D finite difference time domain (FDTD) model for ultrasonic measurements of articular cartilage in pulse-echo configuration. Surface profiles obtained from histological images of human cartilage samples were implemented in the model to evaluate the effect of the surface roughness on the ultrasound reflection from the surface. The simulated results were compared with results from experimental measurements in an identical geometry. Furthermore, artificially created surface profiles with different roughnesses and material parameters were implemented into the model to evaluate systematically their respective contributions to the ultrasound reflection. Finally, the effects of nonperpendicular angle of incidence of the ultrasound beam were studied numerically to simulate the uncertainties related to the experimental measurements.

II. Materials and Methods

A. Sample Preparation and Processing

The experimental part of the present study was extracted from our recent study [19]. In that study, human patellae ($n = 14$) from the right knees of cadaveric do-

Manuscript received September 7, 2009; accepted November 23, 2009. Financial support is acknowledged from the Ministry of Education, Finland, to University of Eastern Finland (project 5765); Academy of Finland, University of Kuopio, Finland (project 127198); Jenny and Antti Wihuri Foundation; I-SKTS, Foundation for Advanced Technology of Eastern Finland, the North Savo Fund of the Finnish Cultural Foundation, the National Graduate School of Musculoskeletal Disorders and Biomaterials, and the Päivikki and Sakari Sohlberg Foundation.

The authors are with the Department of Physics, University of Kuopio, Kuopio, Finland (e-mail: erna.kaleva@uef.fi).

J. Töyräs is also with the Department of Clinical Neurophysiology, Kuopio University Hospital and University of Kuopio, Kuopio, Finland.

Digital Object Identifier 10.1109/TUFFC.2010.1493

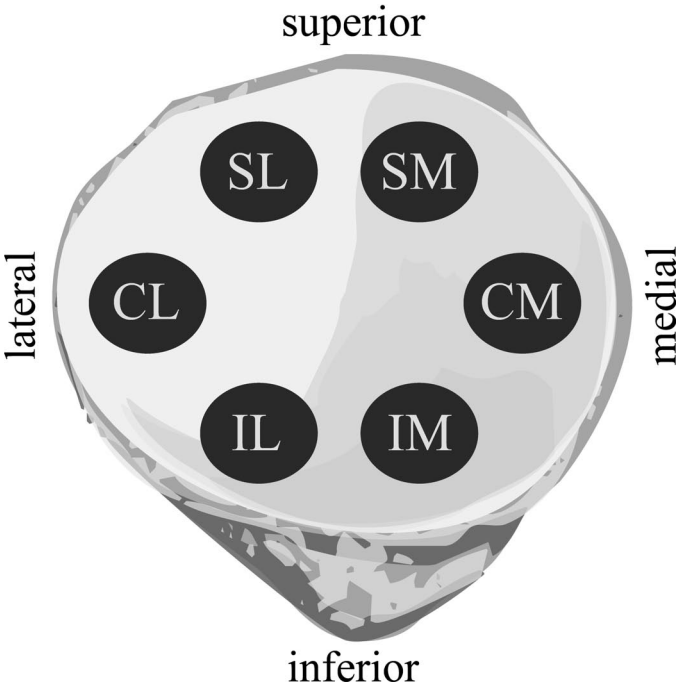

Fig. 1. The ultrasound measurement sites on a human patellar cartilage surface. SL = superolateral, SM = superomedial, CL = central lateral, CM = central medial, IL = inferolateral, and IM = inferomedial.

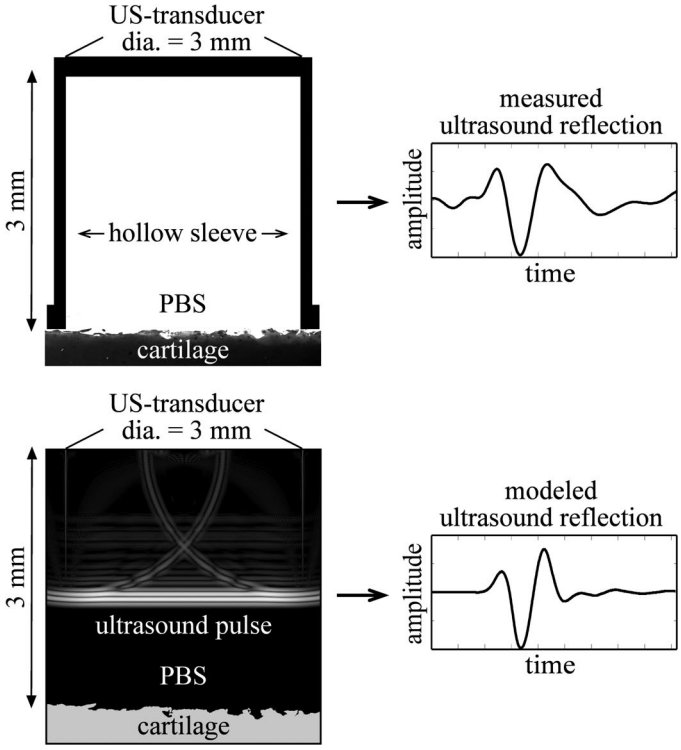

Fig. 2. Schematic presentation (left) of the measurement setup (top) and the model geometry (bottom). Ultrasound signals reflected from the cartilage surface (right) in an experimental measurement (top) and a model simulation (bottom). The cartilage section in the top picture is delineated from an actual histological image. The cartilage section in the bottom picture has been obtained by thresholding the contrast information of the original histological image.

nors (12 males and 2 females, ages from 27 to 79 years, average 56 years) were studied with permission from the National Agency for Mediolegal Affairs in Finland (permission number 1781/32/200/01) [19]. Six measurement sites on medial and lateral facets on each patella were selected: superomedial, superolateral, central medial, central lateral, inferomedial, and inferolateral (Fig. 1). The patellae included cartilage with visually intact appearance and with different grades of surface degeneration related to spontaneous OA [19].

From the total number of $14 \times 6 = 84$ ultrasonic measurement sites, 43 flawless histological sections were prepared, allowing creation of sample-specific models with realistic surface profiles.

B. Ultrasound Reflection Measurements and Analysis

In our recent study, an arthroscopic hand-held indentation instrument [20] equipped with a miniature unfocused 10-MHz ultrasound transducer (XMS310, transducer diameter = 3 mm, near field = 6.9 mm, Panametrics Inc., Waltham, MA) was used to measure the ultrasound reflection from the articular surfaces [19]. A hollow external sleeve was attached to the tip of the instrument to keep the distance between the transducer and the cartilage surfaces constant (3 mm) during the measurements (Fig. 2). Because the inner diameter of the external sleeve was 3 mm, the diameter of the ultrasonic measurement area on the cartilage surface was also 3 mm.

In the present study, the experimental raw data from the earlier study [19] were analyzed to calculate a new parameter. The reflection from a phosphate buffered saline (PBS)-air interface was measured as a reference for the calculation of the integrated reflection coefficient (IRC) [10]. The IRC is defined as

$$\mathrm{IRC} = \frac{1}{\Delta f}\int_{\Delta f} R_c^{\mathrm{dB}}(f)\mathrm{d}f, \tag{1}$$

where Δf is the analyzed frequency range (full width at half of the maximum of the frequency spectrum, 5.3 to 15.5 MHz in this study) and

$$R_c^{\mathrm{dB}}(f) = 10\log_{10}\left\langle\left|\frac{S_c(z,f)}{S_r(z,f)}\right|^2\right\rangle, \tag{2}$$

is a frequency-dependent reflection coefficient where the brackets indicate an average over 3 successive point measurements. The frequency spectra S_c and S_r of the reflections from the PBS-cartilage and the PBS-air interfaces at a distance z, respectively, were obtained by conducting a fast Fourier transform on time domain ultrasound signals that were delimited by a rectangular window. The mixed linear model [21] was used to test the significance of spatial variation in the $\mathrm{IRC}_{\mathrm{exp}}$ values separately within the healthy and degenerated cartilage sample groups. Samples with possible interrelations—in this case, samples

TABLE I. THE COMBINATIONS OF VALUES OF THE MATERIAL PARAMETERS USED IN THE MODEL FOR THE ARTIFICIALLY CREATED SAMPLES.

Material	E (MPa)	v_l (m/s)	v_t (m/s)	ρ (kg/m^3)	λ (MPa)	μ (MPa)	ν
1	**10**	**1525**	**133**	**1010**	**2342.7**	**3.3**	**0.499**
2	20	1550	129	1020	2438.2	6.7	0.499
3	30	1575	131	1030	2536.5	10.0	0.498
4	40	1600	137	1040	2637.7	13.4	0.498
5	**50**	**1625**	**144**	**1050**	**2741.8**	**16.7**	**0.497**
6	60	1650	152	1060	2848.8	20.0	0.497
7	70	1675	159	1070	2958.7	23.4	0.496
8	80	1700	167	1080	3071.7	26.7	0.496
9	90	1725	174	1090	3187.7	30.1	0.495
10	**100**	**1750**	**181**	**1100**	**3306.9**	**33.4**	**0.495**

Young's modulus E, longitudinal velocity v_l, transversal velocity v_t, and density ρ were used to calculate the Lamé constants λ and μ and the Poisson's ratio v. The viscous damping parameters η (shear viscosity) and ϕ (bulk viscosity) were set to constant values of 1.75 N·s/m^2 and 199.7 $\times$ 10^{-6} N·s/m^2, respectively.
The materials selected for evaluation of the angular dependence of ultrasound reflection are in bold.

prepared from the same patella—can be tested with the mixed linear model.

C. Histological Imaging

In our earlier study [19], after the ultrasound imaging, Safranin O stained histological sections (thickness = 3 μm) were prepared from as close to the actual measurement site as possible and imaged using an optical microscope (Nikon Microphot FXA, Nikon Corporation, Tokyo, Japan) equipped with a CCD camera (Nikon CoolSNAP, Nikon Corporation, Tokyo, Japan). In the present study, the surface profiles of the cartilage samples were extracted from the digitized histological sections by tracing the abrupt changes in the contrast between the cartilage and the background. The contrast threshold was manually selected for each sample because the level of Safranin O staining and, to some extent, the background lighting varied between the samples. The reconstructed surface profiles were always visually compared with the original histological images by superimposing semitransparent figures to confirm their correspondence.

D. Modeling

A finite difference model for ultrasound reflection from the cartilage was constructed using Wave 2000 Plus 3.00 R3 software (CyberLogic Inc., New York, NY). The Wave software solves an acoustic differential equation within each homogenous grid element and computes the displacement vector at each time step of the simulation:

$$\rho \frac{\partial^2 \mathbf{w}}{\partial t^2} = \left|\mu + \eta \frac{\partial}{\partial t}\right| \nabla^2 \mathbf{w} + \left|\lambda + \mu + \phi \frac{\partial}{\partial t} + \frac{\eta}{3}\frac{\partial}{\partial t}\right| \nabla(\nabla \cdot \mathbf{w}), \tag{3}$$

where $\mathbf{w}$ is a 2-D displacement vector, t = time [s], ρ = material density [kg/m^3], λ = first Lamé constant [N/m^2], μ = second Lamé constant [N/m^2], η = shear viscosity [N·s/m^2], ϕ = bulk viscosity [N·s/m^2], ∂ = the partial difference operator, ∇^2 = the Laplace operator, and $\nabla\cdot$ = the divergence operator. Isotropy and elasticity of the material are assumed.

The model geometry, identical with the experimental geometry, comprised of a nonfocused 10-MHz ultrasound transducer (diameter = 3 mm) and single-phasic homogeneous cartilage material (distance from transducer = 3 mm) immersed in PBS (Fig. 2). The roughness profiles of the samples, obtained from the digitized histological sections, were implemented in the model individually for each sample. The signal waveform of the transducer was digitized from the datasheet of the XMS-310 10-MHz transducer used in the experimental measurements. A grid size of 3.57 μm was used in the computer simulations, enabling modeling of propagation of ultrasound containing frequencies up to about 15.5 MHz.

The material parameters were chosen so that they correspond to the realistic range of the material parameters of articular cartilage (Table I). The selected range of the longitudinal velocity v_l was from 1525 m/s to 1750 m/s [22]–[24]. The transversal (shear) velocity v_t varied between 133 and 181 m/s. The ultrasound attenuations ranged from 0.7 to 1.1 dB/cm in the longitudinal direction and from 482.5 to 3048.1 dB/cm in the transversal direction within the different materials. The density ρ of the cartilage was estimated to range between 1010 kg/m^3 and 1100 kg/m^3 [25]. Dynamic (instantaneous) moduli from about 2 MPa [26] to about 240 MPa have been reported [27]. Based on this, Young's modulus E was set to vary between 10 MPa and 100 MPa for the ultrasound measurements.

The first and second Lamé constants λ and μ were calculated using the values of E, v_l, v_t, and ρ (Table I) and implemented into the model. The Poisson ratio (ν = 0.495 to 0.499) was calculated to ensure that the implemented values were realistic and that the cartilage was nearly incompressible. The viscous damping parameters η (shear viscosity) and ϕ (bulk viscosity) were set to 1.75 N·s/m^2 and 199.7 $\times$ 10^{-6} N·s/m^2, respectively, based on attenua-

TABLE II. VALUES OF THE IRC_{MODEL} AS A FUNCTION OF THE SURFACE ROUGHNESS FOR THE DIFFERENT COMBINATIONS OF THE VALUES OF THE MATERIAL PARAMETERS PRESENTED IN TABLE I.

	Roughness (μm)						
Material	0.0	5.1	7.8	13.1	26.2	28.8	29.7
1	**−24.0**	**−27.5**	**−27.0**	**−36.6**	**−37.5**	**−36.4**	**−35.4**
2	−20.2	−23.6	−23.3	−35.4	−36.7	−33.9	−34.2
3	−17.3	−20.7	−20.6	−33.9	−33.6	−32.4	−31.0
4	−15.2	−18.5	−18.5	−32.7	−32.0	−31.0	−28.7
5	**−13.4**	**−16.8**	**−16.9**	**−31.1**	**−31.2**	**−28.9**	**−26.9**
6	−12.0	−15.3	−15.5	−29.7	−30.6	−27.4	−25.3
7	−10.8	−14.0	−14.3	−28.7	−30.7	−25.9	−23.9
8	−9.8	−12.9	−13.2	−27.8	−29.3	−24.6	−22.7
9	−8.8	−12.1	−12.4	−27.0	−28.0	−23.8	−21.8
10	**−8.0**	**−11.3**	**−11.6**	**−26.4**	**−26.9**	**−22.8**	**−20.8**

The materials selected for evaluation of the angular dependence of ultrasound reflection are in bold.

tion values presented in literature [23], [24]. The modeling was divided into 3 separate sections as described next.

1) Roughness of the Cartilage Surface: To evaluate systematically the effect of the roughness of the cartilage surface on the integrated reflection coefficient IRC, 7 artificial roughness profiles were generated with Matlab v.7.6.0 (MathWorks Inc., Natick, MA) using a randomized algorithm. The input values for the algorithm included the width of the profile to be created, the desired roughness value and a tolerance limit, the maximum change in the step size (d) and the number of the divisions (n). The width of the profile was randomly divided into n (= 4) sections. For each section, a random vector containing the values of the surface height was created from left to right, step by step. Within every step, the maximum change in the height compared with the previous step was allowed to be ± d (= 4) pixels. Finally, the vectors for each section were combined and the roughness value of the combined vector was checked to confirm that the desired roughness was obtained.

The IRC_{model} was calculated from the modeled (ultrasound simulated) data obtained for the 7 roughnesses with 10 different combinations of the values of the material parameters E, v_l, v_t, and ρ.

2) Ultrasound Angle of Incidence: Three combinations of the values of the material parameters E, v_l, v_t, and ρ were selected (in bold in Table I) to study the effect of the angle of incidence of the ultrasound beam. The aforementioned 7 artificial roughness profiles were inclined by steps of 1° from −5° to 5°, the 0° corresponding to normal incidence of the ultrasound beam. Again, the IRC_{model} was evaluated.

3) Integrity of the Cartilage Surface: One representative digitized histological human cartilage section per sample ($n = 43$, width = 3.5 mm) was selected after visually evaluating all 9 sections made from one sample. The section was implemented into the model to simulate the reflection of the ultrasound from cartilage surfaces with visually intact appearance and with different grades of osteoarthritic surface degeneration. The surface profiles were adjusted to be horizontal by aligning a linear fit of the profile with the horizontal axis. The RMS-roughness values of the cartilage surfaces were determined after filtering out the natural contours of the articular surfaces with a smoothing spline fit [14]. Young's modulus E was assigned individually to each cartilage sample based on the experimentally obtained values from our earlier study [19]. The density ρ of the cartilage and the longitudinal velocity v_l were fixed at 1000 kg/m^3 and 1600 m/s, respectively. Finally the IRC_{exp} was calculated.

III. RESULTS

The dependence of the IRC_{model} on roughness of the surface of the cartilage was approximately similar with different material parameter combinations (Table II). When the roughness of the surface of the cartilage was increased from 0 μm to ∼30 μm, the change in the values of the IRC_{model} was −8 to −14 dB for any chosen combination of the values of the material parameters. To obtain the same change in the values of the IRC_{model} by changing the values of the material parameters, Young's modulus E would have to be changed by about 80 MPa, the longitudinal velocity v_l by about 200 m/s, and the density ρ by about 80 kg/m^3 (Table II).

To show that the simulation code can reproduce analytical results, numerically obtained results were compared with analytical results with the roughness value 0 μm. Because analytical determination of the IRC is not feasible, the time domain reflection coefficient R was used for the validation instead (linear regression analysis between the R and the IRC: $r = 1.000$, $P < 0.01$). Although the analytical reflection coefficient—$R = (Z_{cartilage} - Z_{PBS})/(Z_{cartilage} + Z_{PBS})$, Z = acoustic impedance—does not take into account the viscous component, its values differed from the numerical (simulated) reflection coefficient ($R = A_{cartilage}/A_{reference}$, A = peak-to-peak amplitude) on average only about 2.5% with the different combinations of values of the material parameters.

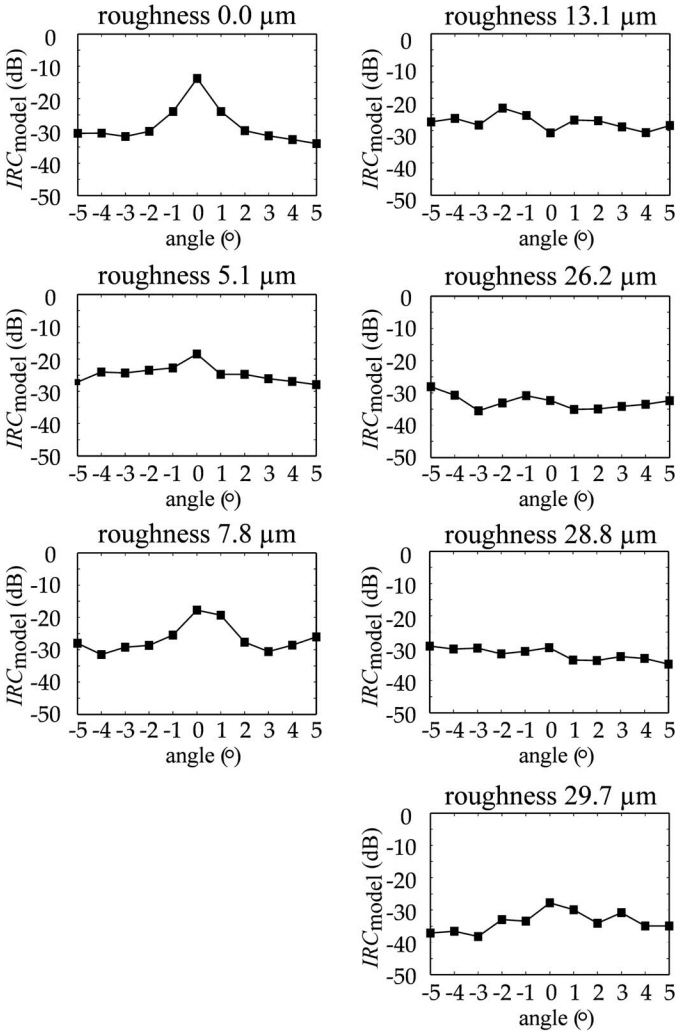

Fig. 3. Angular dependence of the IRC_{model} for different values of surface roughness. For the small roughnesses (0–7.8 μm), the angular dependence is clearly visible. With the rougher surfaces (13.1–29.7 μm), the angular dependence seems to disappear.

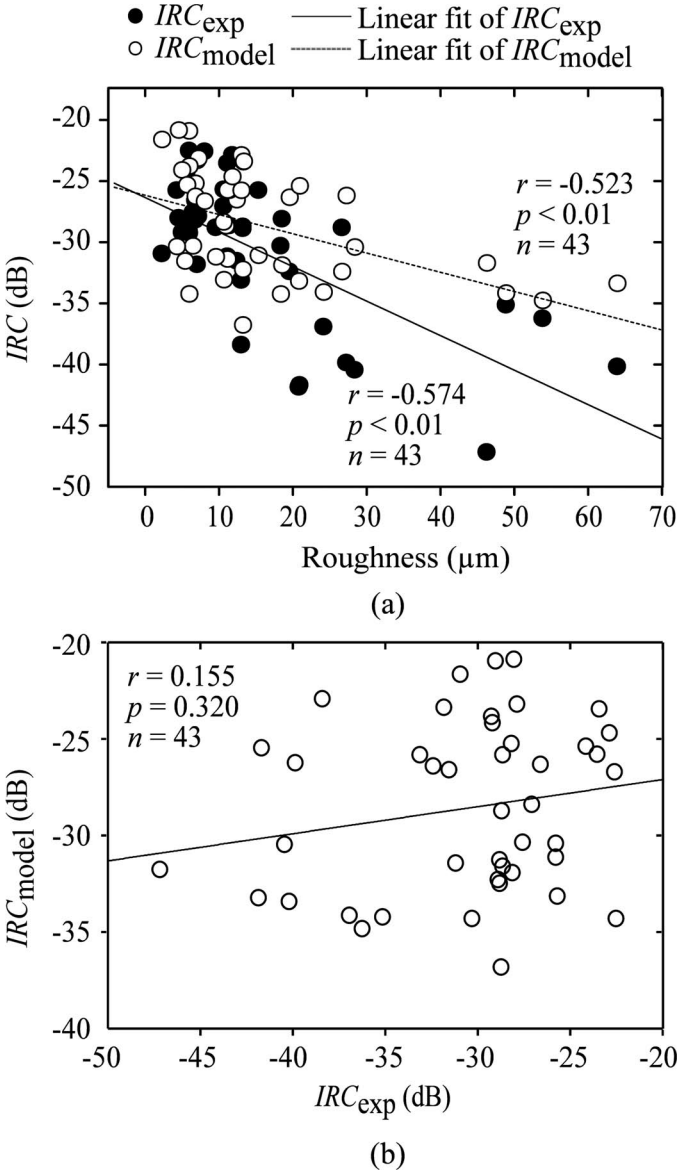

Fig. 4. The linear correlations between (a) the roughness of the human cartilage surface and the experimentally evaluated IRC_{exp} or the numerically evaluated IRC_{model}, (b) the IRC_{exp} and the IRC_{model}.

For the perfectly smooth cartilage surface, the angular dependence of the ultrasound reflection amplitude was apparent (Fig. 3). A threshold between the roughness values 7.8 μm and 13.1 μm was found, beyond which, when the roughness increased, the reflection of the ultrasound at the normal angle of incidence diminished and the angular dependence of the reflection seemed to disappear (Table II, Fig. 3).

There was no site-dependent variation in the IRC_{exp} values of the intact cartilage samples (mixed linear model, $0.294 < P < 0.901$) or the degenerated cartilage samples (mixed linear model, $0.091 < P < 0.975$) and, thus, the results from all 6 measurement sites were pooled. The correlation between the experimentally evaluated IRC_{exp} and the roughness of the human samples was significant ($r = -0.574$, $P < 0.01$); see Fig. 4(a). Also, the numerically evaluated IRC_{model} for the same samples correlated significantly with the roughness ($r = -0.523$, $P < 0.01$); see Fig. 4(a). However, there was no significant correlation between the experimentally and numerically determined values of the IRC ($r = 0.155$, $P = 0.320$); see Fig. 4(b).

IV. Discussion

In this study, an FDTD model for ultrasound reflection from the surface of articular cartilage was constructed. The model was used to evaluate the effects of varying surface roughness, values of material parameters, and ultrasound angle of incidence on the ultrasound reflection. The ultrasound reflection was evaluated using the data from the sample-specific model, and the results were compared with the experimental results obtained in an identical measurement geometry.

The roughness values selected for the artificially created cartilage surface profiles were in the range from 0 to 30 μm, corresponding to the roughness values reported for early degeneration of cartilage [11], [12], [14], [28], [29]. The absolute change in the $\mathrm{IRC}_{\mathrm{model}}$ values between the smooth (roughness = 0 μm) and rough (roughness ≈30 μm) cartilage was about −8 to −14 dB, regardless of the values of the parameters defining the cartilage material (Table II). The human cartilage samples in this study had roughness values in the range from 2 to 64 μm and included samples with a healthy appearance and with signs of early or advanced degeneration. For the human samples, a range from −15 to −25 dB in the changes of the $\mathrm{IRC}_{\mathrm{exp}}$ and the $\mathrm{IRC}_{\mathrm{model}}$ was observed when the roughness was varied from 0 μm to about 30 μm; see Fig. 4(a). The variation in the roughness of the human cartilage surface accounts partly for the changes in the $\mathrm{IRC}_{\mathrm{exp}}$ ($r = -0.574$) and the $\mathrm{IRC}_{\mathrm{model}}$ ($r = -0.523$); see Fig. 4(a). However, the lack of correlation between the $\mathrm{IRC}_{\mathrm{exp}}$ and the $\mathrm{IRC}_{\mathrm{model}}$ ($r = 0.155$), as shown in Fig. 4(b), suggests that the material parameters also contribute significantly to the value of the IRC.

To attain the same range in the change of the $\mathrm{IRC}_{\mathrm{model}}$ (−8 to −14 dB) as by changing the roughness from 0 to 30 μm, Young's modulus E had to be decreased by about 80 MPa, the longitudinal velocity v_l by about 200 m/s, and the density ρ by about 80 kg/m^3 (Table II). Corresponding to a narrow roughness range (e.g., 1 μm), there can be many different values of the experimental $\mathrm{IRC}_{\mathrm{exp}}$; see Fig. 4(a). This suggests that the absolute values of the IRC are affected by the intrinsic material properties of the cartilage. The results for the human samples show that the water content and, thus, the density ρ probably had a great impact on the IRC, because in the model, the density of the human samples was fixed, and in the experimental measurements, its value varied.

When the roughness of the cartilage surface was increased, the angular dependence of the $\mathrm{IRC}_{\mathrm{model}}$ disappeared between the roughness values 7.8 μm and 13.1 μm (Fig. 3). Our previous experimental work indicated the existence of such a boundary value between roughnesses 4.8 and 26.9 μm [18]. The results of the present study support the finding of the earlier study [18], i.e., that scattering may be a more dominant phenomenon than the specular reflection at the surface of degenerated cartilage. In the present study, a threshold of about 2° in the ultrasound angle of incidence was found, beyond which the values of the $\mathrm{IRC}_{\mathrm{model}}$ seemed to even out (Fig. 3). This suggests that if the angle of incidence of the ultrasound beam is not carefully controlled in the measurements, the reliability of the ultrasound diagnosis might be compromised.

Cartilage is a poroviscoelastic, inhomogeneous, and anisotropic material, the acoustical properties of which depend on the composition and structure of the tissue. In the present model, the structure and composition of the cartilage tissue were simplified considerably. Effects of assuming homogeneity and isotropy were probably reduced in the present study because only the ultrasound reflection from the surface of the cartilage was considered. Furthermore, in our model, the shear wave, i.e., transversal ultrasound wave, was considered negligible compared with the longitudinal wave. This assumption was probably reasonable, because the absorption of shear waves in soft tissues is much greater than that of longitudinal waves [30], [31]. This is especially true for cartilage tissue that may contain about 80% water. An obvious limitation of the present model is that it is 2-D, and consequently cannot fully represent a real 3-D measurement situation. The modeling was limited to 2 dimensions for practical reasons, because a corresponding 3-D model with a voxel size of (3.57 μm)^3 ≈45 μm^3 and a transducer-sample distance of 3 mm would have required more than 40 GB of random access memory.

Although the model presented here is not readily applicable as a reference method for experimental ultrasonic measurements, it takes the first fundamental steps on the road toward more realistic acoustic models of articular cartilage and possible model applications in the development of clinical ultrasonic methods. In the future, we aim to develop a 3-D model for ultrasound scattering from articular cartilage. Inclusion of tissue anisotropy and depth-dependent material properties could produce a more realistic acoustic model for cartilage. In osteoarthritis, the changes in the cartilage are accompanied by changes in the subchondral bone such as an increase in the bone volume fraction [32]. Therefore, simultaneous ultrasonic evaluation of cartilage and bone may be diagnostically valuable. In the future, we aim to include subchondral bone in the acoustic model. This is feasible, because FDTD modeling of bone has been successfully applied earlier [33]–[37]. An acoustic model including realistically implemented cartilage and bone might enable more accurate interpretation of high-frequency ultrasound measurements.

Acknowledgment

Eveliina Lammentausta, Ph.D., is acknowledged for her extensive participation in the sample preparation and experimental measurements.

References

[1] J. A. Buckwalter and J. A. Martin, "Osteoarthritis," *Adv. Drug Deliv. Rev.*, vol. 58, no. 2, pp. 150–167, May 2006.

[2] J. A. Buckwalter and J. Martin, "Degenerative joint disease," *Clin. Symp.*, vol. 47, no. 2, pp. 1–32, 1995.

[3] V. C. Mow, D. C. Fithian, and M. A. Kelly, "Fundamentals of articular cartilage and meniscus biomechanics," in *Articular Cartilage and Knee Joint Function: Basic Science and Arthroscopy*, J. W. Ewing, Ed. New York: Raven Press Ltd., 1990.

[4] C. A. McDevitt, "Biochemistry of articular cartilage. Nature of proteoglycans and collagen of articular cartilage and their role in ageing and in osteoarthrosis," *Ann. Rheum. Dis.*, vol. 32, no. 4, pp. 364–378, Jul. 1973.

[5] C. G. Armstrong and V. C. Mow, "Variations in the intrinsic mechanical properties of human articular cartilage with age, degeneration, and water content," *J. Bone Jt. Surg., Am. Vol. (CD-ROM. Ed.)*, vol. 64, no. 1, pp. 88–94, 1982.

[6] D. A. Senzig, F. K. Forster, and J. E. Olerud, "Ultrasonic attenuation in articular cartilage," *J. Acoust. Soc. Am.*, vol. 92, no. 2, pp. 676–681, Aug. 1992.
[7] M.-H. Lu, Y. P. Zheng, Q.-H. Huang, C. Ling, Q. Wang, L. Bridal, L. Qin, and A. Mak, "Noncontact evaluation of articular cartilage degeneration using a novel ultrasound water jet indentation system," *Ann. Biomed. Eng.*, vol. 37, no. 1, pp. 164–175, Jan. 2009.
[8] A. Saïed, E. Chérin, H. Gaucher, P. Laugier, P. Gillet, J. Floquet, P. Netter, and G. Berger, "Assessment of articular cartilage and subchondral bone: Subtle and progressive changes in experimental osteoarthritis using 50 MHz echography in vitro," *J. Bone Miner. Res.*, vol. 12, no. 9, pp. 1378–1386, Sep. 1997.
[9] G. A. Joiner, E. R. Bogoch, K. P. Pritzker, M. D. Buschmann, A. Chevrier, and F. S. Foster, "High frequency acoustic parameters of human and bovine articular cartilage following experimentally-induced matrix degradation," *Ultrason. Imaging*, vol. 23, no. 2, pp. 106–116, Apr. 2001.
[10] E. Chérin, A. Saïed, P. Laugier, P. Netter, and G. Berger, "Evaluation of acoustical parameter sensitivity to age-related and osteoarthritic changes in articular cartilage using 50-MHz ultrasound," *Ultrasound Med. Biol.*, vol. 24, no. 3, pp. 341–354, Mar. 1998.
[11] E. H. Chiang, T. J. Laing, C. R. Meyer, J. L. Boes, J. M. Rubin, and R. S. Adler, "Ultrasonic characterization of in vitro osteoarthritic articular cartilage with validation by confocal microscopy," *Ultrasound Med. Biol.*, vol. 23, no. 2, pp. 205–213, 1997.
[12] R. S. Adler, D. K. Dedrick, T. J. Laing, E. H. Chiang, C. R. Meyer, P. H. Bland, and J. M. Rubin, "Quantitative assessment of cartilage surface roughness in osteoarthritis using high frequency ultrasound," *Ultrasound Med. Biol.*, vol. 18, no. 1, pp. 51–58, 1992.
[13] S. Saarakkala, J. Töyräs, J. Hirvonen, M. S. Laasanen, R. Lappalainen, and J. S. Jurvelin, "Ultrasonic quantitation of superficial degradation of articular cartilage," *Ultrasound Med. Biol.*, vol. 30, no. 6, pp. 783–792, 2004.
[14] S. Saarakkala, M. S. Laasanen, J. S. Jurvelin, and J. Töyräs, "Quantitative ultrasound imaging detects degenerative changes in articular cartilage surface and subchondral bone," *Phys. Med. Biol.*, vol. 51, no. 20, pp. 5333–5346, Oct. 2006.
[15] J. E. Wilhjelm, P. C. Pedersen, and S. M. Jacobsen, "The influence of roughness, angle, range, and transducer type on the echo signal from planar interfaces," *IEEE Trans. Ultrason. Ferroelectr. Freq. Control*, vol. 48, no. 2, pp. 511–521, Mar. 2001.
[16] C. P. Brown, S. W. Hughes, R. W. Crawford, and A. Oloyede, "Ultrasound assessment of articular cartilage: Analysis of the frequency profile of reflected signals from naturally and artificially degraded samples," *Connect. Tissue Res.*, vol. 48, no. 6, pp. 277–285, 2007.
[17] J. Töyräs, J. Rieppo, M. T. Nieminen, H. J. Helminen, and J. S. Jurvelin, "Characterization of enzymatically induced degradation of articular cartilage using high frequency ultrasound," *Phys. Med. Biol.*, vol. 44, no. 11, pp. 2723–2733, Nov. 1999.
[18] E. Kaleva, S. Saarakkala, J. Jurvelin, T. Virén, and J. Töyräs, "Effects of ultrasound beam angle and surface roughness on the quantitative ultrasound parameters of articular cartilage," *Ultrasound Med. Biol.*, vol. 35, no. 8, pp. 1344–1351, Aug. 2009.
[19] P. Kiviranta, E. Lammentausta, J. Töyräs, I. Kiviranta, and J. S. Jurvelin, "Indentation diagnostics of cartilage degeneration," *Osteoarthritis Cartilage*, vol. 16, no. 7, pp. 796–804, Jul. 2008.
[20] M. S. Laasanen, J. Töyräs, J. Hirvonen, S. Saarakkala, R. K. Korhonen, M. T. Nieminen, I. Kiviranta, and J. S. Jurvelin, "Novel mechanoacoustic technique and instrument for diagnosis of cartilage degeneration," *Physiol. Meas.*, vol. 23, no. 3, pp. 491–503, Aug. 2002.
[21] H. Brown and R. Prescott, *Applied Mixed Models in Medicine*. New York: John Wiley & Sons Inc., 2006.
[22] J. Töyräs, M. S. Laasanen, S. Saarakkala, M. J. Lammi, J. Rieppo, J. Kurkijärvi, R. Lappalainen, and J. S. Jurvelin, "Speed of sound in normal and degenerated bovine articular cartilage," *Ultrasound Med. Biol.*, vol. 29, no. 3, pp. 447–454, Mar. 2003.
[23] D. H. Agemura, W. D. O'Brien Jr., J. E. Olerud, L. E. Chun, and D. E. Eyre, "Ultrasonic propagation properties of articular cartilage at 100 MHz," *J. Acoust. Soc. Am.*, vol. 87, no. 4, pp. 1786–1791, Apr. 1990.
[24] H. J. Nieminen, J. Töyräs, J. Rieppo, M. T. Nieminen, J. Hirvonen, R. Korhonen, and J. S. Jurvelin, "Real-time ultrasound analysis of articular cartilage degradation in vitro," *Ultrasound Med. Biol.*, vol. 28, no. 4, pp. 519–525, Apr. 2002.
[25] D. Joseph, W. Y. Gu, X. G. Mao, W. M. Lai, and V. C. Mow, "True density of normal and enzymatically treated bovine articular cartilage," in *Trans. Orthop. Res. Soc.* , 1999, vol. 24, p. 642.
[26] M. S. Laasanen, J. Töyräs, R. K. Korhonen, J. Rieppo, S. Saarakkala, M. T. Nieminen, J. Hirvonen, and J. S. Jurvelin, "Biomechanical properties of knee articular cartilage," *Biorheology*, vol. 40, no. 1–3, pp. 133–140, 2003.
[27] L. V. Burgin and M. A. Richard, "Impact testing to determine the mechanical properties of articular cartilage in isolation and on bone," *J. Mater. Sci. Mater. Med.*, vol. 19, no. 2, pp. 703–711, Feb. 2008.
[28] H. Forster and J. Fisher, "The influence of continuous sliding and subsequent surface wear on the friction of articular cartilage," *Proc. Inst. Mech. Eng. H*, vol. 213, no. 4, pp. 329–345, 1999.
[29] R. J. Minns, F. S. Steven, and K. Hardinge, "Osteoarthrotic articular cartilage lesions of the femoral head observed in the scanning electron microscope," *J. Pathol.*, vol. 122, no. 2, pp. 63–70, Jun. 1977.
[30] E. L. Madsen, H. J. Sathoff, and J. A. Zagzebski, "Ultrasonic shear wave properties of soft tissues and tissuelike materials," *J. Acoust. Soc. Am.*, vol. 74, no. 5, pp. 1346–1355, Nov. 1983.
[31] L. A. Frizzell, E. L. Carstensen, and J. F. Dyro, "Shear properties of mammalian tissues at low megahertz frequencies," *J. Acoust. Soc. Am.*, vol. 60, no. 6, pp. 1409–1411, Dec. 1976.
[32] D. Bobinac, J. Spanjol, S. Zoricic, and I. Maric, "Changes in articular cartilage and subchondral bone histomorphometry in osteoarthritic knee joints in humans," *Bone*, vol. 32, no. 3, pp. 284–290, Mar. 2003.
[33] A. Hosokawa, "Development of a numerical cancellous bone model for finite-difference time-domain simulations of ultrasound propagation," *IEEE Trans. Ultrason. Ferroelectr. Freq. Control*, vol. 55, no. 6, pp. 1219–1233, Jun. 2008.
[34] J. J. Kaufman, G. Luo, and R. S. Siffert, "Ultrasound simulation in bone," *IEEE Trans. Ultrason. Ferroelectr. Freq. Control*, vol. 55, no. 6, pp. 1205–1218, Jun. 2008.
[35] A. S. Aula, J. Töyräs, M. A. Hakulinen, and J. S. Jurvelin, "Effect of bone marrow on acoustic properties of trabecular bone—3D finite difference modeling study," *Ultrasound Med. Biol.*, vol. 35, no. 2, pp. 308–318, Feb. 2009.
[36] G. Haïat, F. Padilla, and P. Laugier, "Sensitivity of QUS parameters to controlled variations of bone strength assessed with a cellular model," *IEEE Trans. Ultrason. Ferroelectr. Freq. Control*, vol. 55, no. 7, pp. 1488–1496, Jul. 2008.
[37] Y. Nagatani, K. Mizuno, T. Saeki, M. Matsukawa, T. Sakaguchi, and H. Hosoi, "Numerical and experimental study on the wave attenuation in bone—FDTD simulation of ultrasound propagation in cancellous bone," *Ultrasonics*, vol. 48, no. 6–7, pp. 607–612, Nov. 2008.

Erna Kaleva was born in Iisalmi, Finland, in 1981. She received her M.Sc. degree in physics from the University of Jyväskylä, Jyväskylä , Finland, in 2008, and her Ph.D. degree in medical physics from the University of Kuopio, Kuopio, Finland, in 2009. Currently, she is working as a researcher in the Biophysics of Bone and Cartilage (BBC) research group of the Department of Physics at the University of Kuopio. Her current research interests include experimental and theoretical optimization of quantitative ultrasound imaging of articular cartilage.

Jukka Liukkonen is a graduate student at the University of Kuopio, Kuopio, Finland. He is currently finishing his master's thesis about finite element modeling of articular cartilage.

Juha Töyräs was born in Rovaniemi, Finland, in 1975. He received his M.Sc. and Ph.D. degrees in medical physics from University of Kuopio, Kuopio, Finland, in 1999 and 2001, respectively. Currently, he is a professor of medical physics and engineering in the Department of Physics, University of Kuopio. He also serves as a physicist at the Diagnostic Imaging Centre, Kuopio University Hospital. Dr. Töyräs is the vice-head of the Biophysics of Bone and Cartilage (BBC) research group of the Department of Physics at the University of Kuopio. His current research interests include development of quantitative ultrasound, arthroscopy, and computed tomography methods for diagnostics of osteoporosis and osteoarthrosis.

Simo Saarakkala was born in Kerava, Finland, in 1979. He received his M.Sc. and Ph.D. degrees in medical physics from the University of Kuopio, Kuopio, Finland, in 2005 and 2007, respectively. He was also nominated as adjunct professor in the Department of Physics, University of Kuopio in 2009. His current research interests include development of quantitative ultrasound and optical-based techniques for diagnostics of osteoarthritis and osteoporosis. Dr. Saarakkala also has four years of experience in clinical work as an assistant medical physicist in Mikkeli Central Hospital and Kuopio University Hospital.

Panu Kiviranta completed his M.D. degree at the University of Helsinki, Helsinki, Finland, in 2008. He defended his Ph.D. thesis on diagnostics of early cartilage degeneration at the University of Kuopio, Kuopio, Finland, and received his Ph.D. degree in 2009. He has worked as a researcher at the University of Kuopio and Kuopio University Hospital since 2003. He also worked as a resident in Kuopio University Hospital in 2008 and 2009. Currently, he is a doctor in specific training in general medical practice at Kuopio Health Center, Kuopio, Finland. Dr. Kiviranta is a member of the Finnish Medical Association and the Finnish Medical Society Duodecim.

Jukka S. Jurvelin was born in Mikkeli, Finland, in 1957. He received his M.Sc. and Ph.D. degrees in medical physics from the University of Kuopio, Kuopio, Finland, in 1982 and 1993, respectively. Currently, he is a professor of medical physics in the Department of Physics and served as the vice rector of the University of Kuopio through the end of 2009. He is the head of the Biophysics of Bone and Cartilage (BBC) research group of the Department of Physics at the University of Kuopio. His current research interests include development of quantitative ultrasound, MRI, and X-ray methods for sensitive diagnostics of osteoporosis and osteoarthritis.